Journal of Applied Polymer Science

Characterization and Gas-Permeation Properties of Crosslinked Diacetylene-Containing Polymer Membranes from Ferulic Acid

Shinji Kanehashi,[1] Toshiaki Nagasawa,[1] Miho Kobayashi,[1] Sung Lin Lee,[1] Masaya Nakamura,[1] Shuichi Sato,[1] Miriam F. Beristain,[1,2] Takeshi Ogawa,[2] Tetsuo Miyakoshi,[1] Kazukiyo Nagai[1]

[1]Department of Applied Chemistry, Meiji University, 1-1-1 Higashi-Mita, Tama-Ku, Kawasaki 214-8571, Japan

[2]Instituto de Investigaciones en Materiales, Universidad Nacional Autonoma de Mexico, Apartado Postal 70-360, Ciudad Universitaria, Distrito Federal 04510, Mexico

Correspondence to: K. Nagai (E-mail: nagai@meiji.ac.jp)

ABSTRACT: Thermally and UV crosslinked poly[propargyl(3-methoxy-4-propargyloxy) cinnamate] (PPOF) were investigated in terms of their physical, thermal, optical, and gas-permeation properties. The crosslinked membranes had high gel contents because of the formation of a diacetylene network. The wide-angle X-ray diffraction patterns showed that all of the membranes were amorphous in structure, regardless of the type of crosslinking reaction. The membrane density increased after the crosslinking reaction; this suggested that the free volume of the crosslinked membrane was lower than that of the untreated membranes. Drastic color changes in the membranes were also observed because of the highly conjugated crosslinked network of diacetylene. In addition, the conjugation caused by diacetylene crosslinking led to visible absorption within the range 400–600 nm. The gas permeation of the crosslinked membrane was reduced compared with that of the untreated membranes. In particular, the gas permeability of the thermally crosslinked membrane was lower than that of UV-irradiated membrane. On the basis of this result, the degree of crosslinking by thermal treatment was higher than that of UV irradiation. Hence, the crosslinked PPOF membranes showed improved gas-barrier properties due to the high conjugation of the crosslinked diacetylene network induced by thermal treatment and UV irradiation. © 2013 Wiley Periodicals, Inc. J. Appl. Polym. Sci. 130: 277–286, 2013

KEYWORDS: biopolymers and renewable polymers; crosslinking; films; membranes

Received 6 November 2012; accepted 4 February 2013; published online 14 March 2013
DOI: 10.1002/app.39121

INTRODUCTION

Environmental problems are currently being experienced worldwide; these include global warming caused by an increase in greenhouse gases (including CO_2 from the consumption of fossil fuels, e.g., coal and oil), air pollution, and the depletion of fossil fuels. Thus, a reduction in CO_2 emissions and the consumption of fossil fuels all over the world is an urgent priority. The use of biobased polymer materials (i.e., bioplastics) made from natural resources, which are ecofriendly renewable resources involving plants and nonfood materials, is one of the most effective methods for addressing these environmental challenges.

At present, some of commercially produced biobased polymer materials include poly(lactic acid) (PLA), denatured starch and cellulose, and polyester from microorganisms (e.g., polyhydroxyalkanoates).[1] PLA is the most widely used biobased polymer for packaging, electronic, and automobile applications because it is an environmentally friendly, biodegradable polymer with a low melting point and high moldability.[2–6]

Ferulic acid is a biomass hydroxycinnamic acid derivative, a lignin precursor in plant cell walls, and is obtained from rice bran.[7] Ferulic acid has a wide range of applications, including as an antioxidant,[8–14] discoloration agent in food applications,[15] skin-lightening agent and sunscreen in cosmetics,[16] packaging,[17,18] and an anticancer and antihyperglycemic agent in medicinal and pharmaceutical applications.[19–30] Studies of polymeric materials containing feluric acid have been reported.[30–33] However, the gas-permeation properties of its crosslinked diacetylene polymers have not been reported yet.

Diacetylene-containing polymers generally undergo crosslinking reactions under thermal, photochemical (i.e., UV), or high-pressure treatments.[34–47] Crosslinked diacetylene-containing polymers are insoluble in common organic solvents and cause membrane color changes.[35] The crosslinking reaction is expected to improve the physical and chemical properties of the polymers because of volume contraction in the covalent coupling of adjacent diacetylene units, which leads to an enhanced density.

Several studies have been reported on the synthesis and structural analysis of diacetylene-containing polymers[42–48] and on some of its characteristics, such as gas separation,[43] optical properties,[38,39,44–46] physical properties,[41,44–48] thermal properties,[43–48] and mechanical strength.[39,40] We recently reported on the synthesis and mechanical strength of novel diacetylene-containing polymer from ferulic acid.[34] However, the physical, thermal, optical, and gas-permeation properties of this polymer and its crosslinked polymers have not yet been investigated. In particular, properties such as the gas-barrier properties (i.e., low gas permeability) and thermal stability are important and desirable characteristics in electronic devices, optical materials, and packaging applications. In this study, the characterization and gas-permeation properties of a crosslinked, biobased diacetylene-containing polymer synthesized from ferulic acid was investigated.

EXPERIMENTAL

Chemicals

Ferulic acid (99%), propargyl bromide (80 wt % in toluene), copper(I) chloride, and *N,N,N′,N′*-tetramethylethylenediamine were purchased from Aldrich and were used without further purification. Potassium carbonate, acetone, and *N,N*-dimethylformamide (DMF) were purchased from Junsei Chemical Co., and *o*-dichlorobenzene was obtained from Kanto Chemical Co. The solvents were dehydrated with a well-dried 4-Å molecular sieve before use.

Synthesis

Poly[propargyl(3-methoxy-4-propargyloxy) cinnamate] (PPOF) was prepared according with a previously reported method.[34] It was purified several times by reprecipitation with chloroform/acidified methanol to remove all catalyst traces. The polymerization proceeded via both head-to-tail and head-to-head linking.

Propargyl(3-methoxy-4-propargyloxy) cinnamate: Yield = 62.7% and melting point = 91 ± 1°C. Fourier transform infrared (FTIR; KBr, cm^{-1}): 3290, 3228 (C—H stretching); 2115 (C≡C stretching); 1719, 1708 (C=O stretching); 1631, 1599, 1513, 1467 (benzene C=C stretching); 1457 (CH_2 bending), 1430 (C—O stretching); 1368 (C—O stretching); 1303 (CH_2 bending); 1270 (C—O stretching); 1235 (=C—O—C stretching); 1142 (=C—O—C bending); 1035, 1020 (C—O bending); 858, 806 cm^{-1} (benzene C—H bending). ^{1}H-NMR [hexadeuterated dimethyl sulfoxide (DMSO-d_6), δ, ppm]: 7.70–7.67 (d, 1H), 7.13–7.11 (d, 1H), 7.07 (dd, 1H), 7.05–7.02 (d, 1H), 6.37–6.34 (d, 1H), 4.82–4.80 (d, 4H), 3.90 (s, 3H), 2.54–2.50 (d, 2H). ^{13}C-NMR (DMSO-d_6, δ, ppm) 166.53, 150.59, 150.00, 146.21, 128.77, 123.33, 115.89, 114.26, 111.56, 79.52, 79.23, 78.22, 77.15, 56.82, 56.18, 52.16. Ultraviolet–visible (UV–vis; DMF): λ_{max} = 323± 1.

PPOF: Yield = 92.6%, number-average molecular weight (M_n) = 16,000, weight-average molecular weight (M_w) = 41,000, M_w/M_n = 2.5, and $[\eta]^{30}_{DMF}$ = 0.58 dL/g. FTIR (KBr, cm^{-1}): 1715 (C=O stretching); 1633, 1597, 1508, 1465 (benzene C=C stretching); 1449 (CH_2 bending); 1420 (C—O stretching); 1367 (C—O stretching); 1304 (CH_2 bending); 1263 (C—O stretching); 1231 (=C—O—C stretching); 1136 (=C—O—C bending); 1028 (C—O bending); 845, 805 (benzene C—H bending). ^{1}H-NMR (DMSO-d_6, δ, ppm): 7.67–7.64 (d, 1H), 7.09 (s, 1H), 7.05 (s, 1H), 6.99–6.94 (t, 1H), 6.34–6.29 (d, 1H), 4.87–4.84 (d, 4H), 3.89 (s, 3H). ^{13}C-NMR (DMSO-d_6, δ, ppm): 166.19, 150.37, 149.51, 146.24, 128.86, 123.14, 115.53, 114.15, 111.51, 76.12, 75.79, 70.61, 69.60, 56.95, 55.99, 52.31. UV–vis (DMF): λ_{max} = 323± 1.

Membrane Preparation

The polymer solution was prepared in 2 wt % chloroform. The filtered solution was placed at room temperature overnight to remove some air trapped in the solution and then cast onto glass Petri dishes. The solutions were covered with aluminum foil to prevent an early crosslinking reaction by room light or sunlight during evaporation. The solvent was then allowed to evaporate for 48 h under atmospheric pressure at 23 ± 1°C. The membrane was immersed in methanol for 7 days to remove any residual solvent. The methanol was replaced with fresh methanol every day. The membranes were dried *in vacuo* at 23 ± 1°C for at least 24 h to remove the methanol. The noncrosslinked membrane is called the *untreated PPOF membrane* in this article. The thickness of the membrane was determined with a digital micrometer (model MDC-25MJ, Mitsutoyo Co.) with precision of up to ±1 μm. The average thickness of the membrane was 30 ± 5 μm.

Thermal and UV Crosslinking Reactions

The thermal treatment of the PPOF membranes was carried out in a vacuum oven at up to 200°C for 4 h. These temperatures were below and beyond the exothermic reaction based on the crosslinking between diacetylene groups.[34] The thermally crosslinked membranes are called *PPOF–thermal membranes* in this article. Meanwhile, the UV irradiation of the membrane was conducted at 23 ± 1°C for up to 5 h under a nitrogen atmosphere with a 100-W, water-cooled, high-pressure mercury lamp (UVL-100HA, Riko Kagaku Sangyo, Inc.) as a light source. The maximum energy distribution was 365 nm at a light intensity of 1.8 mW/cm^2. The crosslinked membrane obtained under this method is called the *PPOF–UV membrane* in this article.

Gel Content

The gel content of the PPOF membrane was determined after the crosslinking reaction to evaluate the degree of crosslinking. The crosslinked membranes were immersed into a chloroform solution at 23 ± 1°C for 24 h, and the nonsoluble parts (i.e., crosslinked parts) were filtered and dried *in vacuo* at 23 ± 1°C to remove residual solvent before weighing. The gel content was calculated with the following equation:

$$\text{Gel content } (\%) = \frac{M_1}{M_0} \times 100 \quad (1)$$

where M_1 and M_0 are the weight of the insoluble fraction and the original weight of the crosslinked membranes, respectively.

Polymer Characterization

All of the ^{1}H-NMR and ^{13}C-NMR spectra were recorded at 35°C on a JNM-ECA500 NMR spectrometer operating at 500 MHz with DMSO-d_6. Cross-polarization/magic angle spinning (CP–MAS) solid-state ^{13}C-NMR experiments were

performed on a JNM-ECA400 NMR spectrometer operating at 400 MHz. FTIR spectroscopy was performed on an FTIR-4100 (Jasco Co.) at 23 ± 1°C with KBr.

The molecular weight of PPOF was determined by gel permeation chromatography relative to polystyrene (PS) standards at 40°C on an HLC-8220 (Tosoh Co.) with TSK gel columns (Super AWM-H) and a detector (RI-8220) with DMF as the eluent at a flow rate of 0.3 mL/min. The inherent viscosities were obtained by the dissolution of PPOF in DMF at a concentration of 0.5% w/v with a Cannon–Fenske viscometer at 30°C.

Membrane Characterization

All of the measurements for membrane characterization were performed three times to confirm the reproducibility of the experimental data.

The membrane density was measured by a buoyancy method with calcium nitrate tetrahydrate at 23 ± 1°C.[49]

Wide-angle X-ray diffraction (WAXD) measurements were performed on a Rint 1200 X-ray diffractometer (Rigaku, Co., Ltd.) with a Cu Kα radiation source at a scanning speed of 2°/min at 40 kV and 20 mA at dispersion angles ranging from 3 to 50° at 23 ± 1°C. The radiation wavelength (λ) was 1.54 Å.

Thermogravimetric analysis (TGA) was performed with a Pyris 1 TGA thermogravimetric analyzer (PerkinElmer, Inc.) from 50 to 900°C in a platinum pan at a heating rate of 10°C/min and a flow rate of 60 mL/min under a nitrogen atmosphere with about 1.0 mg of polymer sample. Differential scanning calorimetry was performed on a Diamond differential scanning calorimeter (PerkinElmer, Inc.) with an aluminum pan. The heat scan was conducted from −100 to 250°C at a heating rate of 10°C/min under a nitrogen atmosphere. The glass-transition temperature (T_g) was determined at the midpoint of the glass transition endotherm of the first heating scan.

UV–vis spectra were taken for a 0.1 wt % solution in DMF, whereas a Multi Spec 1500 spectrophotometer (Shimadzu Co.) was used for the films. The membrane chromaticity was determined with a Spectro-Guide 45/0 spectrophotometric colorimeter (BYK Gardner GmbH) with a white background based on ISO 11664. Refractive index measurements were determined on a DR-A1 refractometer (Atago Co., Ltd.) at 589.3 nm and 23 ± 1°C.

Gas Permeation

All of the gas-permeation measurements were performed for at least three polymer membranes to ensure the reproducibility of the experimental results. The gas permeabilities of H_2, O_2, N_2, CO_2, and CH_4 were determined with the constant-volume/variable-pressure method.[50,51] The upstream gas pressure was 76 ± 1 cmHg, whereas the downstream was *in vacuo*. All of the gas permeabilities were assumed to behave ideally at 35°C. The gas-permeation coefficient [P; cm^3 (STP) cm cm^{-2} s^{-1} $cmHg^{-1}$] was determined with the following equation:[50,51]

$$P = \frac{dp}{dt}\frac{273V}{760(273+T)}\frac{1}{A}\frac{1}{p}\ell \tag{2}$$

where dp/dt is the pressure increase at the steady state t, at the steady state, V is the downstream volume (cm^3), T is the temperature (°C), A (cm^2) is the effective membrane area, p is the upstream pressure (cmHg), and ℓ is the membrane thickness (cm). The ideal gas selectivity of gas A over gas B was expressed as the ratio of the permeability coefficient of gas A over that of gas B:

$$\alpha = \frac{P_A}{P_B} \tag{3}$$

RESULTS AND DISCUSSION

On the basis of the ^{1}H-NMR, ^{13}C-NMR, and FTIR results, the polymer structure was confirmed, as shown in Figure 1. The PPOF was soluble in common solvents, such as THF, chloroform, dichloromethane, dimethyl sulfoxide, and DMF. The gel content of the untreated PPOF membrane was 11 wt % because the polymer underwent slow crosslinking, even at 23 ± 1°C, when kept for a prolonged period. The gel content of the crosslinked membranes was dependent on the heating temperature and the UV-irradiation time (Figure 2). Therefore, further experiments were performed with the crosslinked membranes treated at 100 and 150°C or with UV irradiation for 4 h because the gel contents of the crosslinked PPOF–thermal and PPOF–UV membranes were almost 100%.

The crosslinking induced by thermal or UV-light treatment caused the membrane color to change; this indicated the formation of conjugated structures via diacetylene cross-polymerization. Figure 3 presents the membrane color of the crosslinked PPOF membranes. The untreated PPOF membrane showed a light yellow color, whereas the PPOF–thermal membrane treated at 100°C was orange–yellow, and the PPOF–thermal membrane treated at 150°C became red–brown. On the other hand, the untreated PPOF membrane became slightly yellow after UV irradiation. The color indices were measured with a Lab system to evaluate the membrane color change. The membrane brightness index (L^*) varied from 0 to 100. The maximum of 100 corresponds to a perfect brightness, whereas the minimum of 0 corresponds to a perfect block contrast. The redness ($a^* > 0$)/greenness ($a^* < 0$) and yellowness ($b^* > 0$)/blueness ($b^* < 0$) indices have no specific numerical limits. The overall color difference (ΔE^*) was expressed with the L^*, a^*, and b^* indices as follows:[52]

$$\Delta E^* = \sqrt{(\Delta L^*)^2+(\Delta a^*)^2+(\Delta b^*)^2} \tag{4}$$

When the ΔE^* value is higher than 0.5, a membrane color change is visible. The color indices suggested that the redness increased in the PPOF–thermal membrane, whereas the

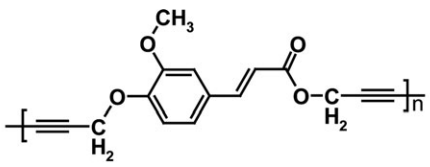

Poly [propargyl (3-methoxy-4-propargyloxy)cinnamate] (PPOF)

Figure 1. Chemical structure of PPOF.

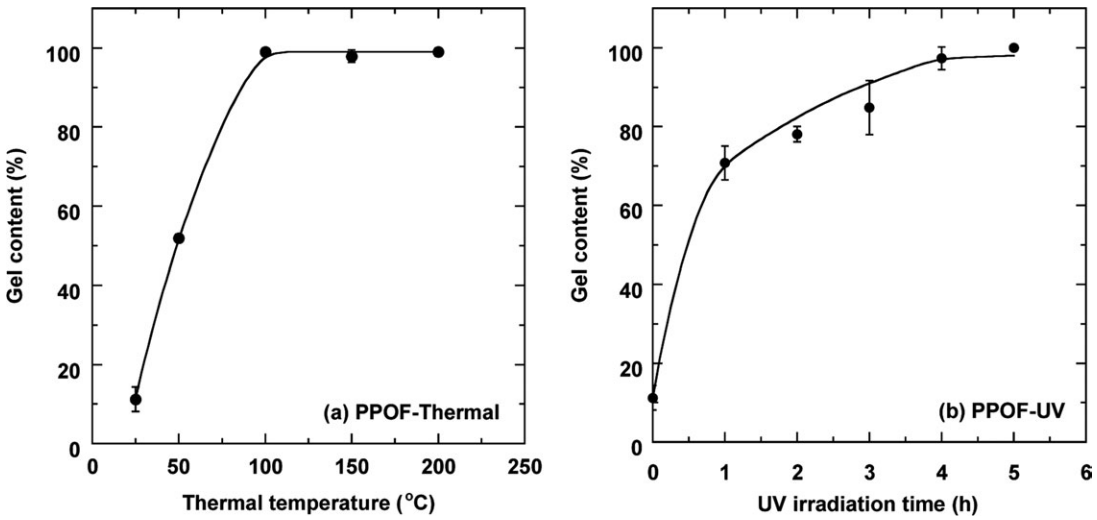

Figure 2. Gel content with increasing (a) temperature and (b) UV-irradiation time for the PPOF membranes.

yellowness increased in the PPOF–UV membrane. On the basis of these color indices, the membrane color was significantly changed after the thermal treatment compared with no treatment. The coloring was due to the formation of conjugated systems by the oligomerization of diacetylenic groups in the main chain by the reaction, as shown in Scheme 1. In addition, the cynnamic double bonds also formed a cyclobutane ring by acetylenic bonds, as shown in Scheme 2.[53] A previous study showed the crosslinking of nontopochemical amorphous aliphatic diacetylene polymers.[54] In our study, the structural change induced by the different crosslink methods was examined on the basis of the membrane solid properties.

The physical properties of the untreated and crosslinked PPOF membranes are shown in Table I. The membrane density of the untreated PPOF was 1.261 g/cm^3, whereas that of the PPOF–thermal and PPOF–UV membranes increased because of the crosslinking reaction between diacetylene units. In particular, the membrane density after thermal treatment at 150°C was higher than those of the other crosslinked membranes; this suggested that the degree of crosslinking was high compared with those of the other membranes. The WAXD patterns of the crosslinked membranes are presented in Figure 4. The untreated PPOF and crosslinked PPOF membranes were amorphous in structure because of their broad

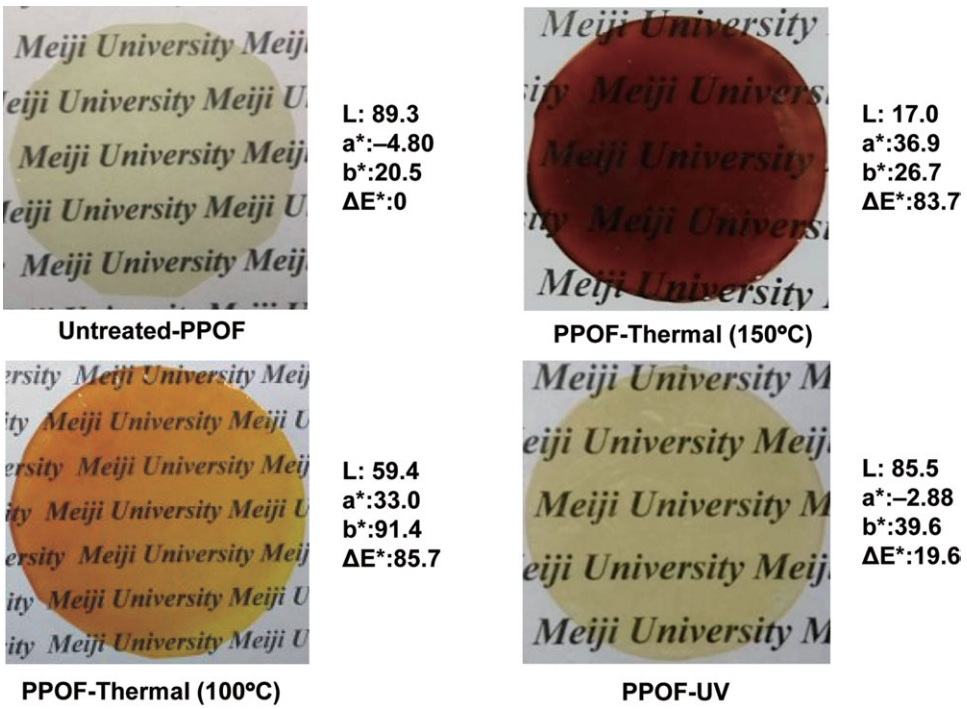

Figure 3. Photographs of the PPOF membranes. [Color figure can be viewed in the online issue, which is available at wileyonlinelibrary.com.]

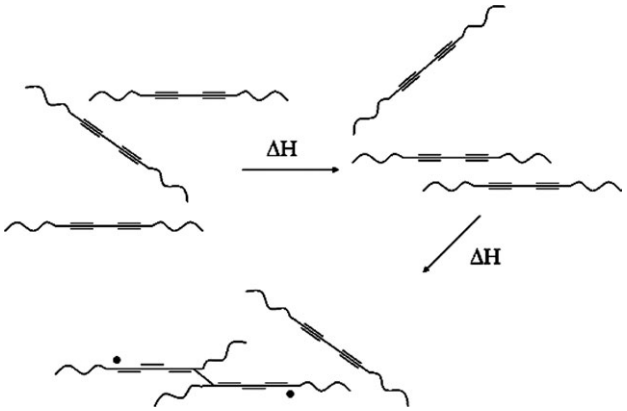

Scheme 1. Mechanism of thermal crosslinking of the amorphous diacetylene-containing polymers.

halo, as shown in Figure 4. The *d*-spacing was calculated with the Bragg equation:[49]

$$\lambda = 2d \sin\theta \quad (5)$$

Only the WAXD pattern of the PPOF–thermal membrane (150°C) showed a widely broad halo with a low intensity. Therefore, the *d*-spacing of the PPOF–thermal membrane (150°C) could not be determined. The patterns of the untreated PPOF, PPOF–thermal (100°C), and PPOF–UV membranes showed two broad halos; the first broad peak at $2\theta = 15.9$–16.8 ($d = 5.2$–5.5 Å) corresponded to the distance between the diacetylene linkage in the adjacent chains, whereas the second broad peak at $2\theta = 23$ ($d = 3.8$ Å) corresponded to the distance between the polymer segments. Interestingly, the *d*-spacing values of these membranes were almost the same, regardless of the crosslinking reaction. This result suggests that the crosslinking reaction could proceed when the distance between the polymer main chains remained constant.

Furthermore, ^{13}C CP–MAS NMR measurements were performed on the PPOF membranes to investigate the structural changes caused by the crosslinking reaction. The CP–MAS spectra of each membrane are presented in Figure 5. Characteristic signals in the untreated PPOF membrane were observed at 55–60 ppm for —CH_2—O— and CH_3—O—, 70–80 ppm for C≡C, 110–140 ppm for C=C and aromatic carbons, 150 ppm for —O—, and 170 ppm for C=O. The crosslinking reaction caused a decrease in the triple bonds from 70 to 80 ppm in all of the

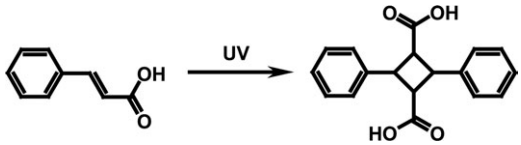

Scheme 2. Mechanism of the photocrosslinking of the amorphous diacetylene-containing polymers.

crosslinked membranes and the appearance of a new signal around 90 to 100 ppm for the PPOF–thermal membrane (150°C), which indicated the formation of a new triple bond characteristic of polydiacetylenes. The enhancement of the peak around 125–130 ppm for the crosslinked membranes resulted from the formation of a double bond (C=C). In addition, a novel peak around 90 ppm in the PPOF–thermal membrane (150°C) appeared; this indicated new bonds formed by the crosslinking reaction between diacetylene groups. On the basis of these results, the thermal and UV-irradiated crosslinking of PPOF gave different crosslinked structures. In addition, the highest degree of crosslinking structure was observed in the PPOF–thermal membrane (150°C). It was reported that the thermal crosslinking reaction takes place via the reaction of diacetylene groups, as shown in Scheme 1, whereas UV radiation at room temperature promotes crosslinking reactions between the photoactive cinnamate moieties and leads to the formation of a cyclobutane ring as a result of [2 + 2] cycloaddition.[53,55,56] Unlike crystalline photoreactive diacetylene-containing polymers, the diacetylene groups must approach each other by the thermal motion of the polymer chains and react to provide diradical species, as shown in Scheme 1. The radicals undergo further reactions, such as the coupling and abstraction of propargyl hydrogen, and the resulting radicals react with each other to form highly crosslinked structures. When sufficient crosslinks are formed, the polymer becomes hard, and the molecular motion stops. Therefore, the polymer still contains a substantial amount of unreacted diacetylene groups after heating.

Thermal Properties

The T_g of the untreated PPOF membrane was around 56°C.[34] The exothermic reaction of the diacetylene groups in the untreated membrane started at 130°C in the first heating scan. On the other hand, obvious endothermic peaks based on the polymer glass transition for the crosslinked membranes were not observed. This was because the random crosslinking reaction between diacetylene groups restricted the mobility of the

Table I. Physical Properties of the Crosslinked PPOF Membranes

Polymer membrane	Crosslinking conditions	Thickness (μm)	Gel content (wt %)	ρ (g/cm^3)	*d*-spacing (Å)		Refractive index
					First	Second	
Untreated PPOF	—	29 ± 2	11 ± 3	1.261 ± 0.001	5.23 ± 0.05	3.75 ± 0.04	1.678 ± 0.002
PPOF-thermal	100°C, 4 h	30 ± 3	99 ± 1	1.287 ± 0.001	5.50 ± 0.17	3.85 ± 0.08	1.664 ± 0.007
PPOF-thermal	150°C, 4 h	31 ± 7	98 ± 1	1.330 ± 0.001	Not applicable		1.647 ± 0.001
PPOF-UV	Room temperature,4 h	31 ± 1	94 ± 6	1.269 ± 0.001	5.50 ± 0.56	3.80 ± 0.14	1.674 ± 0.002

Applied Polymer SCIENCE

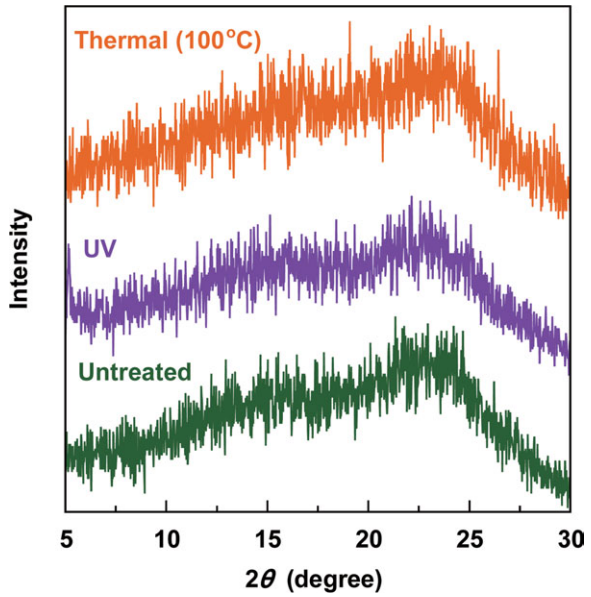

Figure 4. WAXD patterns of the PPOF membranes. [Color figure can be viewed in the online issue, which is available at wileyonlinelibrary.com.]

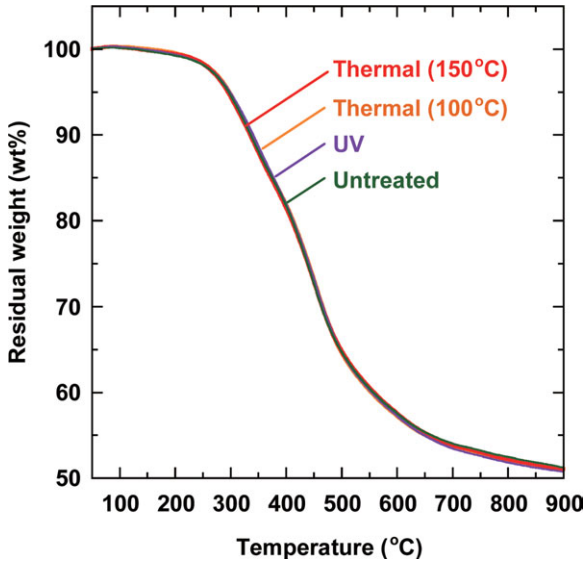

Figure 6. TGA curves of the PPOF membranes. [Color figure can be viewed in the online issue, which is available at wileyonlinelibrary.com.]

polymer chain. In addition, only the PPOF–thermal membrane (150°C) did not show an exothermic reaction based on the crosslinking reaction; this indicated that the reaction was complete under the thermal treatment at 150°C. On the other hand, the crosslinking reaction of the PPOF–thermal (100°C) and PPOF–UV membranes did not proceed completely because the exothermic reaction was still observed.

Figure 6 shows the TGA curves for each PPOF membrane. Interestingly, similar thermal decomposition behavior was observed for all of the PPOF membranes, regardless of their crosslinking reactions. This result indicates that the new linkages between the diacetylene groups in the crosslinked membranes did not affect the thermal stability. This was because the polymer main chains could begin to decompose at 250°C. Therefore, there was no obvious difference in the thermal stability for all of the membranes, regardless of their crosslinking reactions.

Optical Properties

The UV–vis spectra of the membranes were obtained and are shown in Figure 7. The presence of diacetylene groups was evidenced by the absorption band at 254 nm.[41] Interestingly, this band remained nearly constant after the crosslinking reactions;

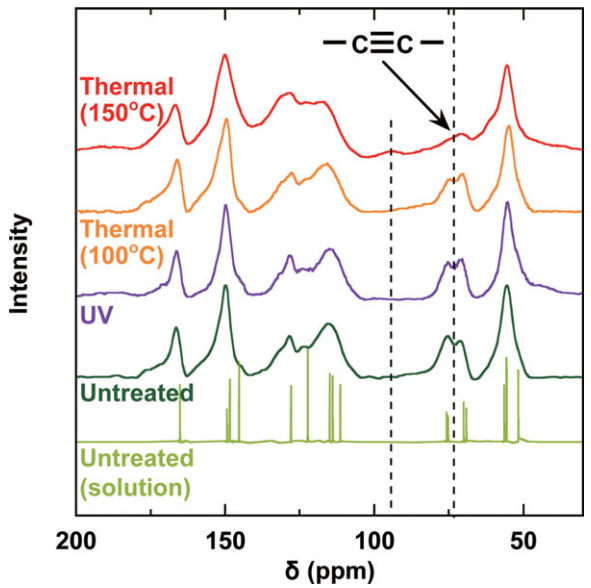

Figure 5. ^{13}C CP–MAS spectrum of the PPOF membranes. [Color figure can be viewed in the online issue, which is available at wileyonlinelibrary.com.]

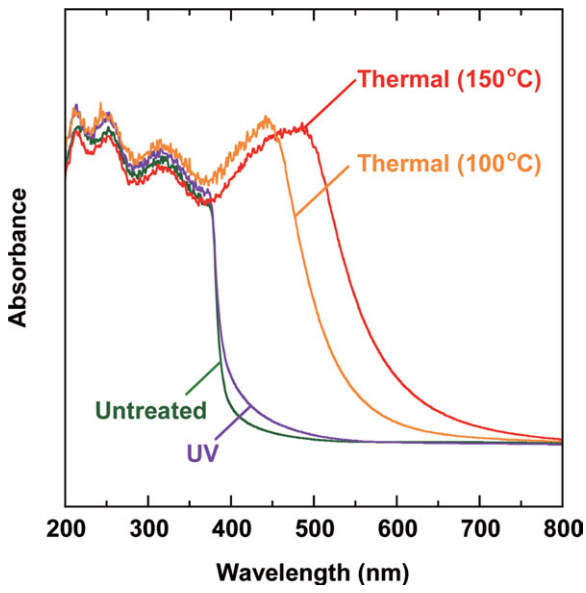

Figure 7. UV–vis spectra of the PPOF membranes. [Color figure can be viewed in the online issue, which is available at wileyonlinelibrary.com.]

Table II. Gas Permeabilities of the Crosslinked PPOF Membranes at 35°C

Polymer membrane	Crosslinking condition	Permeability [cm^3(STP) cm cm^{-2} s^{-1} $cmHg^{-1}$ $\times 10^{-10}$]				
		H_2	O_2	N_2	CO_2	CH_4
Untreated PPOF	—	3.39 ± 0.32	0.118 ± 0.007	0.0221 ± 0.0020	0.598 ± 0.046	0.0142 ± 0.0001
PPOF-thermal	100°C, 4 h	2.09 ± 0.03	0.0503 ± 0.0041	0.00843 ± 0.00028	0.288 ± 0.011	0.00546 ± 0.00040
PPOF-thermal	150°C, 4 h	—	—	—	—	—
PPOF-UV	Room temperature, 4 h	2.72 ± 0.13	0.0908 ± 0.0044	0.0128 ± 0.0003	0.427 ± 0.017	0.00849 ± 0.00043

this indicated the formation of a new triple bond in the crosslinked polymers. For the PPOF–thermal membranes (100 and 150°C), the appearance of a new broad band was observed from 400 to 800 nm, with maximum absorption bands at 450 and 490 nm, respectively. This result was attributed to an increase in π delocalization along the highly crosslinked diacetylene network, which was responsible for the color changes of the membranes,[57] whereas the crosslinked PPOF–UV membranes were not observed. Although the gel content of PPOF–UV was almost 100%, this result also suggested that the low conversion of the diacetylene crosslinking reaction took place under UV irradiation. Therefore, the PPOF membrane was more susceptible to thermal crosslinking via diacetylene units than to UV irradiation.

The refractive indices of the crosslinked membranes at 589 nm are summarized in Table I. The crosslinking reaction resulted in a slight decrease in the refractive index. For example, the refractive indices of the crosslinked membranes were approximately 0.014 for the PPOF–thermal membrane (100°C), 0.31 for the PPOF–thermal membrane (150°C), and 0.004 for the PPOF–UV membrane. These results were attributed to the changes in the conjugated crosslinked network of the diacetylene units obtained by different methods, such as thermal treatment or UV irradiation. As discussed previously, the high free volume of polymers is related to decreases in the refractive index.[45] The order of the refractive indices of the crosslinked membranes was Untreated PPOF > PPOF–UV > PPOF–thermal (100°C) > PPOF–thermal (150°C). However, the physical properties of the crosslinked membranes showed membrane densification compared with the untreated PPOF membrane, as presented in Table I; this indicated that the free volume could decrease after the crosslinking reaction.

Gas-Permeation and Separation Properties

The results of the gas-permeation measurements at 35°C for all of the PPOF membranes are summarized in Table II. The gas permeability of the PPOF–thermal membrane (150°C) was difficult to determine because the membrane was brittle. The order of the gas-permeability coefficients of each PPOF membrane

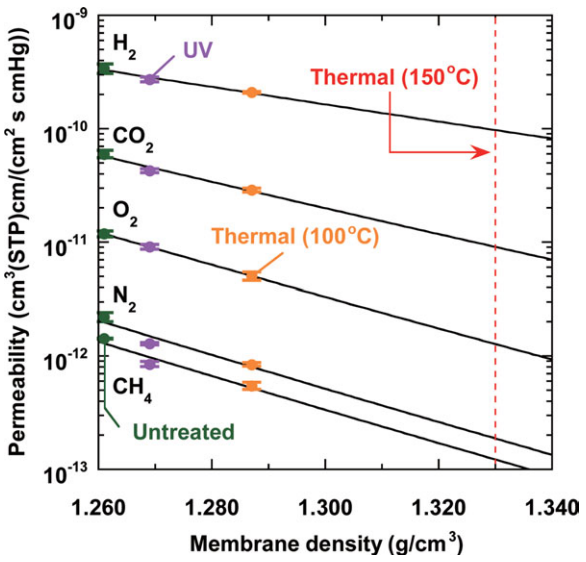

Figure 8. Gas-permeability coefficients as a function of the membrane density in the PPOF membranes. From left to right are the untreated membranes, UV-treated membranes, and thermally treated membranes at 100°C. [Color figure can be viewed in the online issue, which is available at wileyonlinelibrary.com.]

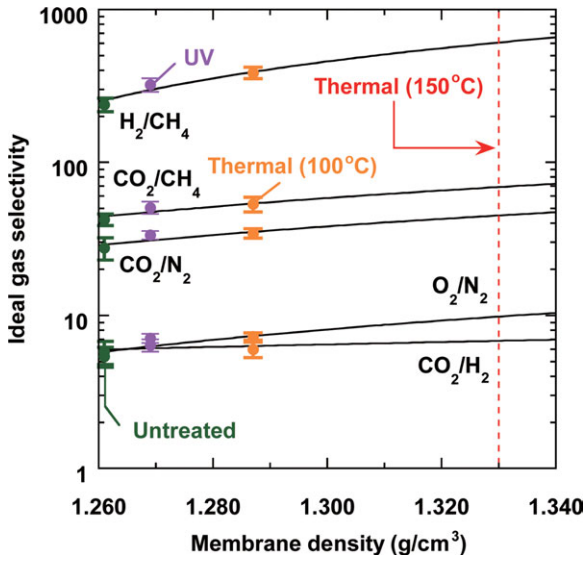

Figure 9. Ideal gas selectivities as a function of the membrane density in the PPOF membranes. From left to right are the untreated membranes, UV-treated membranes, and thermally treated membranes at 100°C. [Color figure can be viewed in the online issue, which is available at wileyonlinelibrary.com.]

Table III. Gas Selectivities of the Crosslinked PPOF Membranes at 35°C

Polymer membrane	Crosslinking conditions	Gas selectivity				
		H_2/CH_4	H_2/CO_2	O_2/N_2	CO_2/N_2	CO_2/CH_4
Untreated PPOF	—	239 ± 24	5.8 ± 1.0	5.4 ± 0.8	27.5 ± 4.6	42.2 ± 3.6
PPOF-thermal	100°C, 4 h	386 ± 34	7.3 ± 0.4	6.0 ± 0.7	34.3 ± 2.5	53.2 ± 5.9
PPOF-thermal	150°C, 4 h	—	—	—	—	—
PPOF-UV	Room temperature, 4 h	322 ± 32	6.4 ± 0.6	7.1 ± 0.5	33.4 ± 2.1	50.6 ± 4.6

was the same for all gases: $P_{H2} > P_{CO2} > P_{O2} > P_{N2} > P_{CH4}$. This order did not follow the gas size; for example, the gas critical volumes were as follows: 65.0 cm^3/mol for H_2, 73.4 cm^3/mol for O_2, 90.1 cm^3/mol for N_2, 94.1 cm^3/mol for CO_2, and 98.6 cm^3/mol for CH_4.[58] At the same time, the order was not consistent with the gas condensability; for example, the gas critical temperatures were 304 K for CO_2, 191 K for CH_4, 155 K for O_2, 126 K for N_2, and 33.3 K for H_2.[58] These results suggest that the gas-permeability coefficients for all of the membranes did not depend on either the diffusivity or solubility but on the balance between the two properties. The order of gas permeability was as follows: Untreated PPOF > PPOF–UV > PPOF–thermal (100°C). This was the same as that of membrane density. As mentioned previously, the decrease in the refractive index of the membranes could have been related to the increase in free volume.[45] However, opposite trend was observed in the crosslinked PPOF membranes. This reason may have been related to the crosslinking reaction between the acetylene groups.

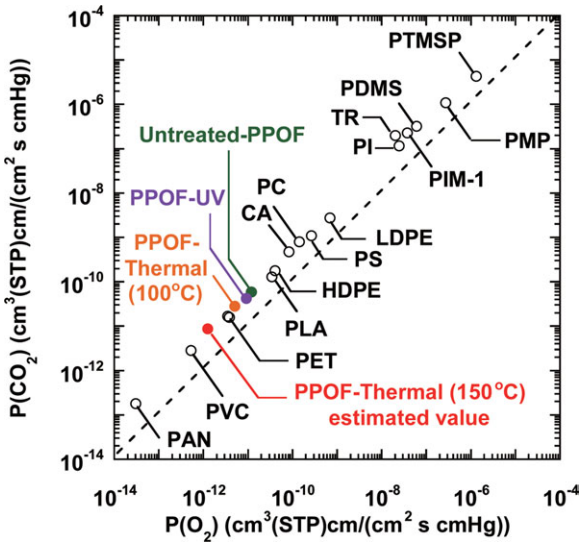

Figure 10. Relationship between the CO_2 and O_2 permeability coefficients in various polymer membranes. The figure includes poly(1-trimethylsilyl-1-propyne) (PTMSP),[59] poly(4-methyl-2-pentyne) (PMP),[62] polydimethylsiloxane (PDMS),[61] 5,5′,6,6′-tetrahydroxy-3,3,3′,3′-tetramethyl-1,1′-spirobisindane-tetrafluoro-terephthalonitrile (PIM-1),[63] thermally rearranged polymer [TR; 4,4-hexafluoroisopropyliden diphthalic anhydride-2,2′-bis (3-amino-4-hydroxylphenyl) hexafluoropropane],[64] 6FDA–2,3,5,6-tetramethylphenylendiamine (PI),[65] low-density polyethylene (LDPE),[61] PS,[61] polycarbonate (PC),[61] cellulose acetate (CA),[61] high-density polyethylene (HDPE),[61] PLA,[5] PPOF, PET,[61] poly(vinyl chloride) (PVC),[61] and polyacrylonitrile (PAN).[61] [Color figure can be viewed in the online issue, which is available at wileyonlinelibrary.com.]

The gas permeability of each PPOF membrane as a function of membrane density is presented in Figure 8. Although the gas permeability of the PPOF–thermal membrane (150°C) could not be measured because the membrane was brittle, the estimated data are plotted in Figure 8. The estimated gas permeability was lower than that of the other crosslinked membranes. Therefore, the crosslinking reaction with thermal treatment in diacetylene-containing polymer membranes were an effective approach for enhancing the gas-barrier properties in this study.

The ideal gas selectivities at 35°C for all of the membranes are summarized in Table III. The gas selectivity determined from the *P* values of the crosslinked membranes increased with increasing membrane density, as presented in Figure 9. For example, the O_2/N_2 selectivity of the untreated PPOF membrane was 5.4, whereas those of the PPOF–thermal membrane (100°C) and PPOF–UV membrane were 6.0 and 7.1, respectively. The increase in the gas selectivity could have been due to the difference in the gas diffusivity produced by the crosslinking reaction. Therefore, the crosslinking in diacetylene units improved the gas-barrier performance and gas selectivity and was observed as a general trade-off relationship.

Figure 10 shows a comparison of the relationships between the CO_2 and O_2 permeabilities of the PPOF membrane and those of other existing conventional polymer membranes.[5,59–64] As shown by this result, the gas permeabilities of the PPOF membranes were higher than that of poly(ethylene terephthalate) (PET), which is widely used in barrier applications, and were lower than those of PS and PLA membranes, which are widely used as packaging materials. In addition, the estimated gas permeability for the PPOF–thermal membrane (150°C) was lower than that for PET. Therefore, the thermal and photochemical crosslinking reactions of diacetylene polymer membranes effective ways to improve their gas-barrier properties because of the highly crosslinked networks between the acetylene groups.

CONCLUSIONS

The physical, thermal, and optical properties of novel diacetylene polymer membranes synthesized from ferulic acid were investigated with a focus on thermal and UV crosslinking reactions. The crosslinked membranes showed high gel contents because of the formation of a diacetylene network. The

membrane density of the PPOF membrane increased after the crosslinking reaction. The increase in the membrane density for the thermally treated membranes was larger than that for UV-irradiated membrane; this suggested that the degree of crosslinking by thermal treatment was higher than that of UV irradiation. Drastic color changes after the crosslinking reaction were also observed in the crosslinked membranes. These results were due to the highly conjugated crosslinked network of diacetylene. Moreover, the conjugation that resulted from diacetylene crosslinking led to visible absorption within the range 400–600 nm. The gas-permeation properties of the PPOF membranes were also lower than that of PLA, which is also fabricated from biomass. Furthermore, the gas permeabilities of the PPOF membranes decreased with the crosslinking reactions as a result of the diacetylene network. Therefore, the thermally and UV-irradiation-induced crosslinking reactions of diacetylene polymer membranes constitute an effective approach for improving the gas-barrier properties.

ACKNOWLEDGMENTS

This research was partially supported by Research Project Grant B (3) from the Institute of Science and Technology, Meiji University, Japan. One of the authors (T.O.) acknowledges DGAPA–UNAM (Dirección General de Asuntos del Personal Académico) for financial support (contract grant number IT100112).

REFERENCES

1. Pilla, S. Handbook of Bioplastics and Biocomposites Engineering Applications; Wiley-Scrivener, **2011**.
2. Dorgan, J. R.; Braun, B.; Wegner, J. R.; Knauss, D. M. Degradable Polymers and Materials; American Chemical Society: Washington, DC, **2006**.
3. Serizawa, S.; Inoue, K.; Iji, M. *J. Appl. Polym. Sci.* **2006**, *100*, 618.
4. Shen, L.; Worrell, E.; Patel, M. *Biofuels Bioprod. Bioref.* **2010**, *4*, 25.
5. Sawada, H.; Takahashi, Y.; Miyata, S.; Kanehashi, S.; Sato, S.; Nagai, K. *Trans. Mater. Res. Soc. Jpn.* **2010**, *35*, 241.
6. Sato, S.; Ono, M.; Yamauchi, J.; Kanehashi, S.; Ito, H.; Matsumoto, S.; Iwai, Y.; Matsumoto, H.; Nagai, K. *Desalination* **2012**, *287*, 290.
7. Zhao, Z.; Moghadasian, M. H. *Food Chem.* **2008**, *109*, 691.
8. Mathew, S.; Abraham, T. E. *Crit. Rev. Biotechnol.* **2004**, *24*, 59.
9. Graf, E. *Free Radical Biol. Med.* **1992**, *13*, 435.
10. Hiroe, K.; Hisamoto, M.; Hirose, K.; Akiyama, K.; Taniguchi, H. *J. Agric. Food Chem.* **2002**, *50*, 2161.
11. Nenadis, N.; Zhang, H.-Y.; Tsimidou, M. Z. *J. Agric. Food Chem.* **2003**, *51*, 1874.
12. Masuda, T.; Yamada, K.; Maekawa, T.; Takeda, Y.; Yamaguchi, H. *J. Agric. Food Chem.* **2006**, *54*, 6069.
13. Anselmi, C.; Centini, M.; Granata, P.; Sega, A.; Buonocore, A.; Bernini, A.; Facino, R. M. *J. Agric. Food Chem.* **2004**, *52*, 6425.
14. Trombino, S.; Serini, S.; Di Nicuolo, F.; Celleno, L.; Andò, S.; Picci, N.; Calviello, G.; Palozza, P. *J. Agric. Food Chem.* **2004**, *52*, 2411.
15. Maoka, T.; Tanimoto, F.; Sano, M.; Tsurukawa, K.; Tsuno, T.; Tsujiwaki, S.; Ishimaru, K.; Takii, K. *J. Oleo. Sci.* **2009**, *57*, 1749.
16. Murray, J. C.; Burch, J. A.; Streilein, R. D.; Iannacchione, M. A.; Hall, R. P.; Pinnell, S. R. *J. Am. Acad. Dermatol.* **2008**, *59*, 418.
17. Mathew, S.; Abraham, T. E. *Food Hydrocolloids* **2008**, *22*, 826.
18. Cao, N.; Fu, Y.; He, J. *Food Hydrocolloids* **2007**, *21*, 575.
19. Jung, E. H.; Ran Kim, S.; Hwang, I. K.; Youl Ha, T. *J. Agric. Food Chem.* **2007**, *55*, 9800.
20. Ardiansyah, Y. O.; Shirakawa, H.; Koseki, T.; Komai, M. *J. Agric. Food Chem.* **2008**, *56*, 2825.
21. Mori, H.; Kawabata, K.; Yoshimi, N.; Tanaka, T.; Murakami, T.; Okada, T.; Murai, H. *Anticancer Res.* **1999**, *19*, 3775.
22. Hudson, E. A.; Dinh, P. A.; Kokubun, T.; Simmonds, M. S. Gescher, A. *Cancer Epidemiol. Biomarkers Prev.* **2000**, *9*, 1163.
23. Cheng, C.-Y.; Su, S.-Y.; Tang, N.-Y.; Ho, T.-Y.; Chiang, S.-Y.; Hsieh, C.-L. *Brain Res.* **2008**, *1209*, 136.
24. Mohmmad Abdul, H.; Butterfield, D. A. *Biochim. Biophys. Acta* **2005**, *1741*, 140.
25. Cho, J.-Y.; Kim, H.-S.; Kim, D.-H.; Yan, J.-J.; Suh, H.-W.; Song, D.-K. *Prog. Neuropsychopharmacol. Biol. Psychiatry* **2005**, *29*, 901.
26. Jin, Y.; Yan, E. Z.; Fan, Y.; Zong, Z. H.; Qi, Z. M.; Li, Z. *Acta. Pharmacol. Sin.* **2005**, 943.
27. Perluigi, M.; Joshi, G.; Sultana, R.; Calabrese, V.; De Marco, C.; Coccia, R.; Cini, C.; Butterfield, D. A. *J. Neurosci. Res* **2006**, *84*, 418.
28. Yan, J.-J.; Cho, J.-Y.; Kim, H.-S.; Kim, K.-L.; Jung, J.-S.; Huh, S.-O.; Suh, H.-W.; Kim, Y.-H.; Song, D.-K. *Br. J. Pharmacol.* **2001**, *133*, 89.
29. Koh, P.-O. *Neurosci. Lett.* **2012**, *507*, 156.
30. Puoci, F.; Iemma, F.; Curcio, M.; Parisi, O. I.; Cirillo, G.; Spizzirri, U. G.; Picci, N. *J. Agric. Food Chem.* **2008**, *56*, 10646.
31. Du, J.; Fang, Y.; Zheng, Y. *Polymer* **2007**, *48*, 5541.
32. Castillo, E. A.; Miura, H.; Hasegawa, M.; Ogawa, T. *Design. Monom. Polym.* **2004**, *7*, 711.
33. Elias, H.-G.; Palacios, J. A. *Makromol. Chem.* **1985**, *186*, 1027.
34. Beristain, M. F.; Nakamura, M.; Nagai, K.; Ogawa, T. *Des. Monomer Polym.* **2009**, *12*, 257.
35. Wegner, V. G. *Makromol. Chem.* **1970**, *134*, 219.
36. Hay, A. S.; Bolon, D. A.; Leimer, K. R.; Clark, R. F. *J. Polym. Sci. Polym. Lett. Ed.* **1970**, *8*, 97.
37. Day, D.; Lando, J. B. *J. Polym. Sci. Polym. Lett. Ed.* **1981**, *19*, 227.
38. Pons, M.; Johnston, D. S.; Chapman, D. *Biochem. Biophys. Acta* **1982**, *693*, 461.

39. Liang, R.-C.; Reiser, A. *J. Polym. Sci. Part A: Polym. Chem.* **1987**, *25*, 451.
40. Beckham, H. W.; Rubner, M. F. *Polymer* **1991**, *32*, 1821.
41. Beckham, H. W.; Rubner, M. F. *Macromolecules* **1993**, *26*, 5192.
42. Gerasimov, G. N.; Popova, E. L.; Phomin, S. M.; Kiryanova, T. V.; Teleshov, E. N. *Macromol. Rapid Commun.* **1995**, *16*, 155.
43. Karangu, N. T.; Rezac, M. E.; Beckham, H. W. *Chem. Mater.* **1998**, *10*, 567.
44. Tregre, G. J.; Mathias, L. J. *J. Polym. Sci. Part A: Polym. Chem.* **1997**, *35*, 587.
45. Badarau, C.; Wang, Z. Y. *Macromolecules* **2004**, *37*, 147.
46. Soules, A.; Ameduri, B.; Boutevin, B.; Calleja, G. *Macromolecules* **2010**, *43*, 4489.
47. Hu, X.; Li, X. *J. Polym. Sci. Part B: Polym. Phys.* **2002**, *40*, 2354.
48. Kolel-Veetil, M. K.; Beckham, H. W.; Keller, T. M. *Chem. Mater.* **2004**, *16*, 3162.
49. Kanehashi, S.; Nakagawa, T.; Nagai, K.; Duthie, X.; Kentish, S.; Stevens, G. *J. Membr. Sci.* **2007**, *298*, 147.
50. Komatsuka, T.; Kusakabe, A.; Nagai, K. *Desalination* **2008**, *234*, 212.
51. Komatsuka, T.; Nagai, K. *Polym. J.* **2009**, *41*, 455.
52. Polyzois, G. L.; Tarantili, P. A.; Frangou, M. J.; Andreopoulos, A. G. *J. Prosthet. Dent.* **2000**, *83*, 572.
53. Schönberg, A.; Khandelwal, G. D. *Chem. Ber.* **1970**, *103*, 2780.
54. Hernández-Rojas, M. E.; Peralta, E.; Beristain, M. F.; Ogawa, T. *Des. Monomer Polym.* **2010**, *13*, 473.
55. Gupta, P.; Trenor, S. R.; Long, T. E.; Wilkes, G. L. *Macromolecules* **2004**, *37*, 9211.
56. Ichimura, K.; Akita, Y.; Akiyama, H.; Kudo, K.; Hayashi, Y. *Macromolecules* **1997**, *30*, 903.
57. Bloor, D.; Chance, R. R. Polydiacetylenes: Synthesis; Structure and Electronic Properties; Martinus Nijhoff: Dordrecht, The Netherlands, **1985**.
58. Poling, B. E.; Prausnitz, J. M.; O'Connell, J. P. The Properties of Gases and Liquids; McGraw-Hill: New York, **2000**.
59. Nagai, K.; Higuchi, A.; Nakagawa, T. *J. Polym. Sci. Part B: Polym. Phys.* **1995**, *33*, 289.
60. Miyata, S.; Sato, S.; Nagai, K.; Nakagawa, T.; Kudo, K. *J. Appl. Polym. Sci.* **2008**, *107*, 3933.
61. Allen, S. M.; Fujii, M.; Stannett, V.; Hopfenberg, H. B.; Williams, J. L. *J. Membr. Sci.* **1977**, *2*, 153.
62. Morisato, A.; Pinnau, I. *J. Membr. Sci.* **1996**, *121*, 243.
63. Budd, P. M.; Msayib, K. J.; Tattershall, C. E.; Ghanem, B. S.; Reynolds, K. J.; McKeown, N. B.; Fritsch, D. *J. Membr. Sci.* **2005**, *251*, 263.
64. Park, H. B.; Han, S. H.; Jung, C. H.; Lee, Y. M.; Hill, A. J. *J. Membr. Sci.* **2010**, *359*, 11.
65. Kanehashi, S.; Gu, H.; Shindo, R.; Sato, S.; Miyakoshi, T.; Nagai, K. *J. Appl. Polym. Sci.*, to appear.